SEMARAK ILMU PUBLISHING

Journal of Advanced Research in Fluid Mechanics and Thermal Sciences

Journal homepage:
https://semarakilmu.com.my/journals/index.php/fluid_mechanics_thermal_sciences/index
ISSN: 2289-7879

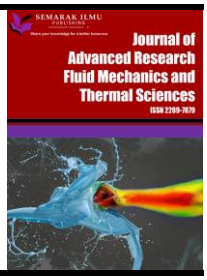

Chemically Radiative and Slip Effects on MHD Heat and Mass Transfer Flow of Maxwell Nanofluid across an Inclined Surface

Gopinathan Sumathi Mini[1], Prathi Vijaya Kumar[1,*], Shaik Mohammed Ibrahim[2], Giulio Lorenzini[3]

[1] Department of Mathematics, GITAM (Deemed to be University), Visakhapatnam, Andhra Pradesh 530045, India
[2] Department of Engineering Mathematics, College of Engineering, Koneru Lakshmaiah Education Foundation, Vaddeswaram, Andhra Pradesh, 522302, India
[3] Department of Engineering and Architecture, University of Parma, Parco Area delle Scienze 181/A 43124 Parma, Italy

ARTICLE INFO

Article history:
Received 10 June 2023
Received in revised form 13 August 2023
Accepted 25 August 2023
Available online 12 September 2023

Keywords:
Upper-convected Maxwell fluid; inclined stretching surface; nonlinear velocity slip; thermal radiation; suction

ABSTRACT

In both the laboratory and the manufacturing setting, nanofluids play a crucial role in improving the thermal properties of pure fluids. The heat and mass transmission of an incompressible upper-convected Maxwell fluid along a stretched sheet in the midst of heat radiation, chemical changes, and suction is investigated. The nonlinear slip condition for the Maxwell fluid is put into account herein. The diffusion model for mass and heat transfer introduced by Cattaneo and Christov is incorporated in the modelling process. The partial differential equations that regulate the system are reduced into a more fundamental form via similarity transformations. Mathematica's NDSolve technique is implemented to do a numerical treatment of the dimensionless equations once they have been translated. The upsides of this strategy lie in its ability to automatically track errors and select the best algorithm. Assessments are taken of velocity, temperature, concentration, skin friction, Nusselt number, and Sherwood number, among others. Graphs are used to quickly illustrate and clarify how various material qualities affect the flow of mass and heat transmission. Thermal relaxation and chemical reaction parameters minimize temperature and concentration fields. It is observed that greater Maxwell parameters implies a rise in the intensity of skin friction, whereas a spike in the slip parameter generates a decrease. Nusselt and Sherwood numbers diminish with Maxwell parameter.

1. Introduction

Over the past few years, scientists and engineers have discovered that adding a modest quantity of nanoparticles can significantly improve the thermal characteristics of the underlying fluids. Boundary layer flows of non-Newtonian as well as Newtonian fluids over stretched surfaces are of relevance in metallurgy, chemical processing, and ecosystems. Nuclear reactor cooling down, packed platform catalytic reactors, fibre and wire coating, processing of food, fluidization in reactors, cooling by evaporation, elevated oil recovery, and reservoirs of geothermal energy are all examples

* *Corresponding author.*
E-mail address: vprathi@gitam.edu

https://doi.org/10.37934/arfmts.109.1.126146

of such programmers. Non-Newtonian fluid activity is evident in a broad spectrum of commercial fluids, including molten polymers, synthetic fibres, blood, polymetric liquids, and food-related substances. Nanofluids are fluids that include nanoparticles, often minerals or oxides of metal. In addition to improving the efficiency of heat transfer, nanoparticles improved the thermo-physical phenomenon. The type of nanoparticle material, shape, scattered particle, and other factors affect how effectively heat is transferred. In nanofluids, thermophoresis and Brownian diffusion are essential slip mechanisms. Non-Newtonian Williamson fluid is a pseudo-plastic fluid that does not rely on the passage of time. Industrial and technological applications of non-Newtonian nanofluid boundary flow on a linear surface include photography and polymer surface extraction. Several nanoparticles, including multi-walled carbon nanotubes (MWCNT), fullerene, copper oxide and silicon dioxide, have been employed to create nanofluids in this work by Hwang *et al.,* [1] to improve thermal conductivity and lubricity. Oil, ethylene glycol and DI water have all been utilised as base fluids. Thermal conductivity has been examined in order to look into the thermo-physical characteristics of nanofluids. Jalili *et al.,* [2] assess the heat transfer processes of the nanofluid stream via the microchannel heat sink with a magnetic field using Al_2O_3-water nanofluid for cooling. Arshad *et al.,* [3] studied viscous nanofluid flow with heat and mass transfer over a porous flat surface in a continuous magnetic field, also Brownian motion, thermophoresis, and viscous dissipation are among the other parameters taken into account. Jalili *et al.,* [4] computationally and theoretically explained the transient squeezing flow of 2D Magnetohydrodynamics (MHD) with Casson fluid under solar irradiance. Tracking the heat and mass transfer phase in the solar irradiance process helps reduce solar unit energy use. This problem assumes temperature-dependent mass and heat diffusivity. Using exponentially expanding sheets to generate magnetic fields, Anwar *et al.,* [5] simulated fluid flow with varying thermal conductivity and investigated the effects of thermophoresis and Brownian motion on viscous dissipation and chemical changes. Esfe and Afrand [6] researched on the techniques for producing nanoparticles and several approaches for figuring out how thermally conductable they are. Reddy and Sreedevi [7] looked at both steady and unsteady instances of nanofluid flow over a stretched surface contained in a porous medium and employed a variety of criteria to infer how heat and mass transfer happened.

Due to its widespread use in engineering and physics, research in Maxwell nanofluid flow on a stretched surface surged recently. Nuclear power plants, aeroplanes, combustion chambers, fuel cells, glass fibre manufacture, and paper producing are all examples of places where these techniques are used. Motsa *et al.,* [8] examine the passage of the magnetohydrodynamic (MHD) boundary layer flow of an incompressible upper-convected Maxwell (UCM) fluid through a porous, stretched surface. While considering the numerical consequences of a large number of parameters, Shateyi and Marewo [9] studied the flow of an upper-convected incompressible Maxwell fluid over a stretched sheet, complete with heat and mass transmission. The continuous laminar boundary layer flow and heat transmission past a stretched sheet were investigated by Hayat *et al.,* [10] treating the Upper convected Maxwell fluid as a rheological model.

Due to its many uses, magnetohydrodynamics with heat, mass, radiation, and diffusion has drawn the attention of many scholars. It is used in astrophysics and geophysics to study star and sun structures, ionosphere radio transmission and other phenomena. Engineering usage include MHD pumps, bearings, and others. Theoretical theories on star structure include mass transfer, which may affect the sun's surface. Free convection flow in liquid metals, electrolytes, and ionised gases depends on magnetic field research. Power engineering is affected by hydromagnetic mass transfer thermal physics. Radiative fluxes occur in industrial and environmental processes. Heating and cooling chambers, fossil fuel combustion, evaporation from enormous open water reservoirs, astrophysical fluxes, solar power technologies and space craft re-entry are examples.An interesting kind of

viscoelastic fluid that may illustrate the characteristics of fluid relaxation time is the upper convected Maxwell fluid. It allows for the emphasis to be placed on the effects of fluid elasticity on the characteristics of its boundary layer while excluding complex effects of shear-dependent viscosity. Kodi *et al.,* [11] studied implications of Dufour's law and variable thermal conductivity in maxwell nanofluid magnetohydrodynamic (MHD) mixed convection flow in a vertical cone with porous material. Several theoretical as well as experimental studies on the thermal conductivity of nanofluids were published and examined in the work by Ahmadi *et al.,* [12]. The effects of thermal emissions on the heat transmission and movement of non-Newtonian fluids in a channel were looked into by Khan *et al.,* [13]. Several aspects affecting mass transfer processes were considered by Shah *et al.,* [14] in their investigation of upper-convected Maxwell (UCM) nanofluid flow across an inclined stretched sheet subject to a magnetic field. With a constant heat flux and a non-uniform heat source and sink, Das [15] investigated the impact of different fluid characteristics on heat and mass transport through an inclined permeable plate. Raghunath [16] studied the heat and mass transfer of an unsteady, MHD incompressible water based nanofluid flow considering thermal radiation effects. Ali *et al.,* [17] investigated how slip impacts magnetohydrodynamic unsteady Maxwell nanofluid flow through a stretched, permeable sheet with heat radiation, thermo-diffusion, and chemical reaction. Numerous industrial processes, such as those used to create polymers or lasers for medical procedures, rely on an understanding of magnetohydrodynamics (MHD) with heat transmission flow via a permeable stretching or shrinking sheet. Raftari and Yildirim [18] employed the homotopy perturbation technique (HPM) to determine the analytic flow through the boundary layer of an upper-convected Maxwell (UCM) fluid via a porous stretched sheet. Farooq *et al.,* [19] used the Buongiorno model to investigate non-Newtonian Maxwell fluids including nanoparticles on an exponentially growing surface. Slip impact on UCM fluid flow was studied by Ibrahim and Negera [20] under conditions of chemical reaction and magnetic field. Three-dimensional fluid over a stretched surface has been investigated by Hayat and Awais [21]. Over a Cattaneo and Christov-modified extended surface heat flux model, Tausif *et al.,* [22] have studied the flow of a nanofluid boundary layer at the surface. Nandeppanavar *et al.,* [23] looked over the flow of a magnetohydrodynamic (MHD) liquid that is incompressible in a two-dimensional boundary layer towards a non-linearly moving flat surface with velocity and temperature slip. Using a Casson nanofluid, heat generation/absorption, and a magnetic field, Narender *et al.,* [24] propose a computer model to investigate implications for the flow near the MHD stagnation point due to radiation. Awan *et al.,* [25] analyzed a two-dimensional stagnation point flow of a poor grade fluid, where the fluid impinges on the oscillatory stretching surface at an angle. The thermal and related properties of a Casson nanofluid near a stagnation region in a porous media were investigated by Kumar *et al.,* [26]. Employing a two-dimensional Darcy-Forchheimer model, Hosseinzadeh *et al.,* [27] studied the chemically reactive radiating flow. Unsteady magnetohydrodynamic Maxwell nanofluid flow with chemical reactions was the focus of a study by Patil *et al.,* [28].

By accounting for thermal and concentration relaxation durations, Cattaneo-Christov double diffusion models generalize Fourier and Fick's equations of heat and mass diffusion. Suction is an approach to boundary layer control that seeks to reduce energy losses in channels and drag on bodies in external flows. Suction is used to enhance the efficiency of diffusers with high working fluid compression ratios (with large convergence angles) by postponing the separation of the boundary layer. Identifying the minimum amount of suction fluid requires to maintain a laminar boundary layer is essential for applying suction because using an excessive amount of suction fluid could considerably increase power consumption, thereby nullifying the power savings from a reduction in drag. Mustafa *et al.,* [29] analyse upper-convected Maxwell (UCM) fluid flow and heat transmission in rotating frames, considering temperature-dependent thermal conductivity fluid. A non-Fourier

heat flux term with thermal relaxation effects models heat transmission and Cattaneo–Christov and Fourier models are also compared. A stretched porous cylinder was studied by Sheikholeslami [30] for nanofluid flow and heat transfer. It was observed that the Nusselt number increases with nanoparticle volume fraction, suction parameter, Reynolds number, and nanofluids. Shah *et al.,* [31] analysed hybrid nanofluid dynamics using type I and type II hybrid models, focusing on the differences and highlighting that Suction and dual stretching affect hybrid nanofluid boundary layer flow [32]. Models chemically reactive Maxwell nanofluid for axisymmetric flow using Cattaneo-Christov heat flux model and updated nanofluid model. Arrhenius activation energy and magnetic field are also mentioned. Omowaye and Animasaun [33] studied an upper-convected Maxwell (UCM) fluid flow over a melting surface situated in hot environment is studied. The influence of melting heat transfer and thermal stratification are properly accounted for by modifying the classical boundary condition of temperature to account for both.

Four novel aspects served as the basis for our current effort. The primary goal of this study was to simulate and analyse the two-dimensional chemically radiative MHD flow of a Maxwell nanofluid. The second objective is to examine the dynamics of this flow over an inclined surface. The third step is to examine characteristics of the slip effects, Brownian motion, and thermophoresis. As a fourth goal, we intend to use the NDSolve method to generate numerical solutions for the velocity, temperature, and concentration fields. Also, graphical analyses of the skin friction coefficient and the local Nusselt and Sherwood numbers have been performed. None of the previous works considered the analysis of the MHD Maxwell nanofluid flow over an inclined surface under these effects using NDSolve. This paper is then an endeavour to fill this gap. As research in this area continues, it is likely that we will see even more applications for these techniques in the future.

2. Mathematical Formulation

A laminar, constant, and incompressible flow of an electrically conducting UCM nanofluid towards an inclined stretching surface has been taken. The surface has an angle Ω relative to the vertical position. Thermal radiation and suction are now taken into consideration in the energy equation.

In order to construct the coordinate axes as seen in Figure 1, the x axis is taken along the flow direction while the y axis is normal to it. Thermophoresis and Brownian motion, as well as the effects of chemical reactions and suction and non-Newtonian velocity slip, have also been considered. The velocity of the stretching sheet has been taken as $u = u_w = ax$. The temperature near and distant from the surface are denoted as T_w and T_∞, respectively, while concentration C_w and C_∞ also respectively. The fluid is subjected to a magnetic field of intensity B_0 that is normal to the flow when the flow analysis is being done.

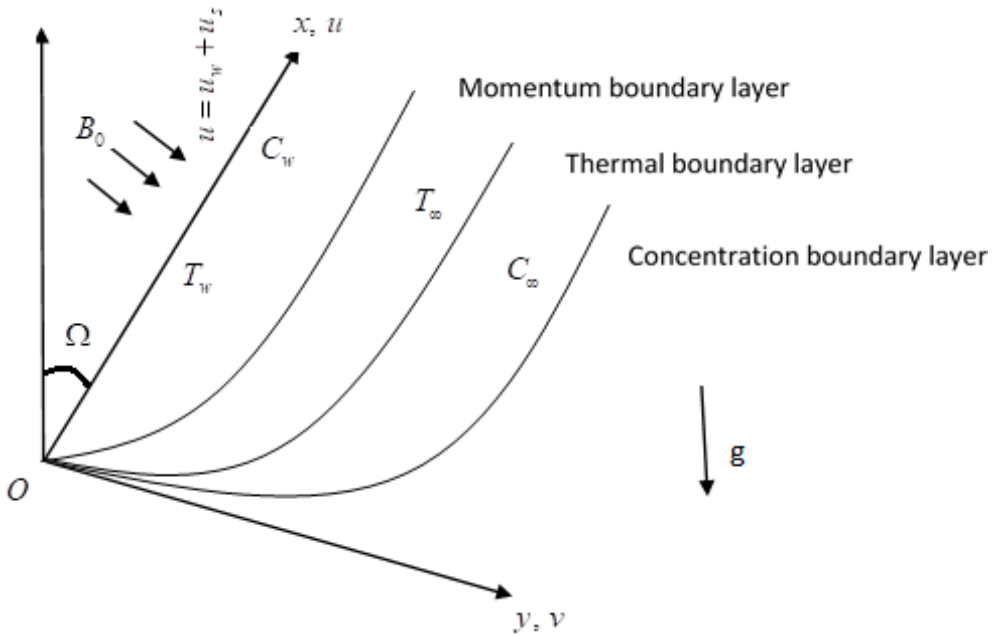

Fig. 1. Physical flow

Under the premise of weak magnetic fields, Reynolds number facilitates ignoring the induced magnetic field. Following are the boundary layer equations given the above mentioned restrictions [33]

$$\frac{\partial u}{\partial x}+\frac{\partial u}{\partial y}=0, \tag{1}$$

$$u\frac{\partial u}{\partial x}+v\frac{\partial u}{\partial y}=v\frac{\partial^2 u}{\partial y^2}-\lambda_f\left(u^2\frac{\partial^2 u}{\partial x^2}+v^2\frac{\partial^2 u}{\partial y^2}+2uv\frac{\partial^2 u}{\partial x\partial y}\right)-\frac{\sigma {B^2}_0}{\rho_f}\left(u+\lambda_f v\frac{\partial u}{\partial y}\right), \tag{2}$$
$$+\left[\left(T-T_\infty\right)\beta_T+\left(C-C_\infty\right)\beta_C\right]g\cos\Omega$$

$$u\frac{\partial T}{\partial x}+v\frac{\partial T}{\partial y}=-\frac{1}{\left(\rho C_p\right)_f}\nabla.\mathbf{q}+\frac{Q_0\left(T-T_\infty\right)}{\left(\rho C_p\right)_f}+\tau\left(D_B\frac{\partial T}{\partial y}\frac{\partial C}{\partial y}+\frac{D_T}{T_\infty}\left(\frac{\partial T}{\partial y}\right)^2\right)-\frac{1}{\left(\rho C_p\right)_f}\frac{\partial q_r}{\partial y}, \tag{3}$$

$$u\frac{\partial C}{\partial x}+v\frac{\partial C}{\partial y}=-\frac{1}{\left(\rho C_p\right)_f}\nabla.\mathbf{J}+D_B\frac{\partial^2 C}{\partial y^2}+\frac{D_T}{T_\infty}\frac{\partial^2 T}{\partial y^2}-K_c\left(C-C_\infty\right), \tag{4}$$

In order to analyse concentration as well as temperature diffusion, in the present research revised versions of Fourier's and Fick's laws have been included. The combined version of the Fourier and Fick's laws, as proposed by the Cattaneo-Christov heat flow theory, looks like this:

$$\mathbf{q}+\lambda_h\left(\frac{\partial \mathbf{q}}{\partial t}+\left(\nabla.\mathbf{V}\right)\mathbf{q}+\mathbf{V}.\nabla\mathbf{q}-\mathbf{q}.\nabla\mathbf{V}\right)=-k_f\nabla T, \tag{5}$$

$$\mathbf{J}+\lambda_m\left(\frac{\partial \mathbf{J}}{\partial t}+(\nabla.\mathbf{V})\mathbf{J}+\mathbf{V}.\nabla\mathbf{J}-\mathbf{J}.\nabla\mathbf{V}\right)=-D_B\nabla C\,, \tag{6}$$

where $\mathbf{V}$ is the velocity field, $\mathbf{q}$ and $\mathbf{J}$ are used, respectively, for the normal heat and mass fluxes. The temperature dependence of the thermal conductivity is assumed to be linear. Using the Taylor series, we can linearize the T^4 in radiative heat flux q_r about T_∞ as follows.

$$\frac{\partial q_r}{\partial y}=-\frac{16{T_\infty}^3\sigma^*}{3k^*}\frac{\partial^2 T}{\partial y^2}, \tag{7}$$

Simplifying the Eq. (3) to Eq. (6) by using incompressibility $\nabla.\mathbf{V}=0$ and the steady flow conditions $\frac{\partial \mathbf{q}}{\partial t}$, $\frac{\partial \mathbf{J}}{\partial t}$ equal to zero we arrive at the following form

$$\begin{aligned}u\frac{\partial T}{\partial x}+v\frac{\partial T}{\partial y}+\lambda_h\left[u^2\frac{\partial^2 T}{\partial x^2}+v^2\frac{\partial^2 T}{\partial y^2}+2uv\frac{\partial^2 T}{\partial x\partial y}+\left(u\frac{\partial u}{\partial x}+v\frac{\partial u}{\partial y}\right)\frac{\partial T}{\partial x}+\left(u\frac{\partial v}{\partial x}+v\frac{\partial v}{\partial y}\right)\frac{\partial T}{\partial y}\right]\\ =\left(\alpha_f+\frac{16{T_\infty}^3\sigma^*}{3k^*\left(\rho C_p\right)_f}\right)\frac{\partial^2 T}{\partial y^2}+\tau\left[D_B\frac{\partial T}{\partial y}\frac{\partial C}{\partial y}+\frac{D_T}{T_\infty}\left(\frac{\partial T}{\partial y}\right)^2\right]+\frac{Q_0\left(T-T_\infty\right)}{\left(\rho C_p\right)_f},\end{aligned} \tag{8}$$

$$\begin{aligned}u\frac{\partial C}{\partial x}+v\frac{\partial C}{\partial y}+\lambda_m\left[u^2\frac{\partial^2 C}{\partial x^2}+v^2\frac{\partial^2 C}{\partial y^2}+2uv\frac{\partial^2 C}{\partial x\partial y}+\left(u\frac{\partial u}{\partial x}+v\frac{\partial u}{\partial y}\right)\frac{\partial C}{\partial x}+\left(u\frac{\partial v}{\partial x}+v\frac{\partial v}{\partial y}\right)\frac{\partial C}{\partial y}\right]\\ =D_B\frac{\partial^2 C}{\partial y^2}+\frac{D_T}{T_\infty}\frac{\partial^2 T}{\partial y^2}-K_c\left(C-C_\infty\right),\end{aligned} \tag{9}$$

The associated boundary conditions are

$$\left.\begin{aligned}&u=u_w+u_s=ax+\Lambda\frac{\partial u}{\partial y}-\lambda_f\left(u\frac{\partial u}{\partial x}-au+v\frac{\partial u}{\partial y}\right),v=-v_w,(T,C)=\left(T_w,C_w\right)\ at\ \ y=0,\\ &u\to 0,\frac{\partial u}{\partial y}\to 0,(T,C)\to\left(T_\infty,C_\infty\right)\ as\ \ y\to\infty.\end{aligned}\right\} \tag{10}$$

Where v_w is the velocity suction (>0) or injection (<0).

The mathematical model is converted into the non-dimensional form using the local similarity transformations listed below:

$$\begin{aligned}&\eta=\sqrt{\frac{a}{\upsilon}}y,\ u=axf'(\eta),\ v=-\sqrt{av}\,f(m),\ \psi=\sqrt{av}\,xf(\eta),\ C-C_\infty=\phi\left(C_w-C_\infty\right),\\ &T-T_\infty=\theta\left(T_w-T_\infty\right),\end{aligned} \tag{11}$$

where ψ is the stream function.

Using the Transformations on Eq. (2), Eq. (8), Eq. (9) we get

$$f''' + \lambda\left(2ff'f'' - f^2 f'''\right) - f'^2 - Mf' + \left(1 + M\lambda ff''\right) + \left(\lambda_t\theta + \lambda_c\phi\right)\cos\Omega = 0, \tag{12}$$

$$\frac{1}{\Pr}\left(1 + (4/3)R\right)\theta'' - \gamma_e\left(f^2\theta'' + ff'\theta'\right) + f\theta' + \left(Nb\theta'\phi' + Nt\theta'^2\right) + Q\theta = 0, \tag{13}$$

$$\phi'' + \frac{Nt}{Nb}\theta'' + Sc\, f\phi' - Sc\,\gamma_c\left(f^2\phi'' + ff'\phi'\right) - Sc\, C_r\phi = 0. \tag{14}$$

Subject to (11) the corresponding boundary conditions becomes

$$\begin{aligned} &f(0) = S,\ f'(0) = 1 + \varepsilon f''(0) - \lambda\left[f'^2(0) - f'(0)\right],\ \theta(0) = 1, \phi(0) = 1, \\ &f'(\eta), \theta(\eta), \phi(\eta) \to 0 \ \ as \ \ \eta \to \infty. \end{aligned} \tag{15}$$

The dimensionless quantities used in Eq. (12) to Eq. (15) are

$$\begin{aligned} &M = \frac{\sigma B^2{}_0}{\rho a}, \lambda_t = \frac{\beta_T\left(T_w - T_\infty\right)g}{a^2 x}, \lambda_c = \frac{\beta_C\left(C_w - C_\infty\right)g}{a^2 x}, Q = \frac{Q_0}{\rho C_p a}, \tau = \frac{(\rho C)_p}{(\rho C)_f}, \\ &Nb = \frac{\tau D_B}{\nu\left(C_w - C_\infty\right)}, \lambda = Gr_x a, Gc_x = \lambda_h a, \varepsilon = \Lambda\sqrt{\frac{a}{\nu}}, Nt = \frac{\tau D_T}{\nu T_\infty\left(T_w - T_\infty\right)}, R = \frac{4T_\infty{}^3\sigma^*}{k_f k^*}, \\ &C_r = \frac{K_c}{a}, \Pr = \frac{\nu}{\alpha_f}, Sc = \frac{\nu}{D_B}, \gamma_c = \lambda_m a, S = \frac{v_w}{\sqrt{a\nu}}. \end{aligned} \tag{16}$$

3. Methodology for Solution

Mathematica's NDSolve package was used to find a solution to the system of non-dimensional standard differential Eq. (12) to Eq. (14) subject to boundary conditions (15).

The above common nonlinear differential equations are numerically solved in this study using Mathematica's NDSolve command. This approach is unconditionally stable and converges. The default convergence criteria for NDSolve are an absolute tolerance of 1e-6 and a relative tolerance of 1e-3. These values are typically sufficient for most problems. The maximum step size 0.01 is used in the current numerical computations to get the numerical solution with six orders of local accuracy for the approach as a criterion of convergence. For evidence of the numerical scheme's preciseness, the latest results of $-\theta'(0)$ and $-\phi'(0)$ are assessed against Shah *et al.,* [34] outcomes in Table 1.

Table 1

Comparison of the numerical values of $-\left(1+\frac{4R}{3}\right)\theta'(0)$ and $-\phi'(0)$ for different values of M, Nb, Nt when
$\lambda = 0.3, \lambda_t = \lambda_c = \varepsilon = 0.1, \gamma_e = \gamma_c = R = 0.5, \Pr = 6.2, Q = 0.2, S = 0.0,$
$Sc = 1.2, C_r = 1.0, \Omega = \pi / 3.$

M	Nb	Nt	Shah *et al.*, [34]		Present Outcomes	
			$-\left(1+\frac{4R}{3}\right)\theta'(0)$	$-\phi'(0)$	$-\left(1+\frac{4R}{3}\right)\theta'(0)$	$-\phi'(0)$
0.5	0.5	0.1	0.564694	1.301828	0.564694	1.301828
1.5	0.5	0.1	0.472342	1.280714	0.472342	1.280714
2.5	0.5	0.1	0.400706	1.266277	0.400706	1.266277
0.5	0.3	0.1	0.953515	1.263584	0.953515	1.263584
0.5	0.7	0.1	0.307091	1.307904	0.307091	1.307904
0.5	0.5	0.2	0.467093	1.347080	0.467093	1.347080
0.5	0.5	0.3	0.384389	1.401479	0.384389	1.401479

4. Results and Discussion

In this section, we look at how the parameters alter the temperature, concentration and flow fields. This was accomplished by using the MATHEMATICA NDSolve function to numerically solve the governing Eq. (11) to Eq. (14) and condition (15). The leading parameters are given fixed values for all computations:

$\lambda = 0.3, M = 0.3, S = \varepsilon = Nt = \gamma_e = \gamma_c = \lambda_t = \lambda_c = 0.1, R = 0.5, \Pr = 6.2, Nb = 0.5, Q = 0.2, Sc = 1.2,$
$C_r = 1.0.$

The impact of the magnetic field M on the velocity and temperature profiles can be witnessed in Figure 2 and Figure 3 respectively. The velocity profile drops as M increases, while the temperature profiles broaden. The Lorentz force always challenges fluid movement and the larger M yields to it. As a result, we see a lessening impact here. The magnetic field also has features that make the temperature profiles better.

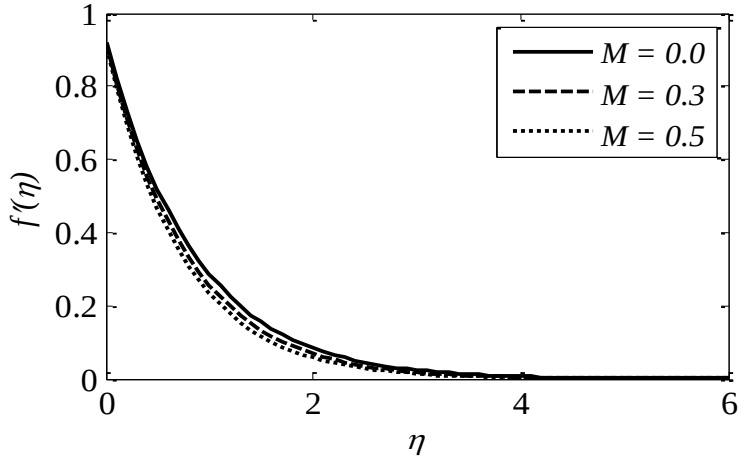

Fig. 2. Effect of M on velocity profile

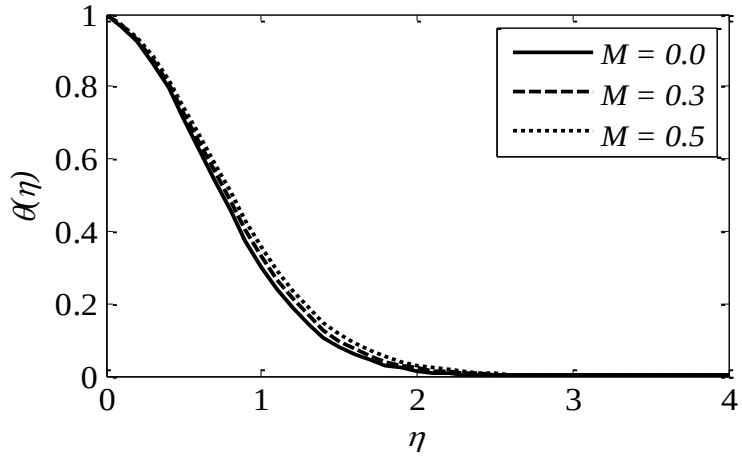

Fig. 3. Effect of M on temperature profile

Figure 4 demonstrates the manner in which the Maxwell parameter λ alters the velocity. When λ gets larger, velocity impedes down. For viscoelastic materials, the Maxwell parameter, or fluid relaxation parameter, is significant. When the Maxwell parameter is petite, the fluid behaves like a Newtonian and viscous one, whereas when it is enormous, the fluid takes on non-Newtonian features. Thus, the velocity as well as its boundary layer thickness alleviate for rising levels of λ.

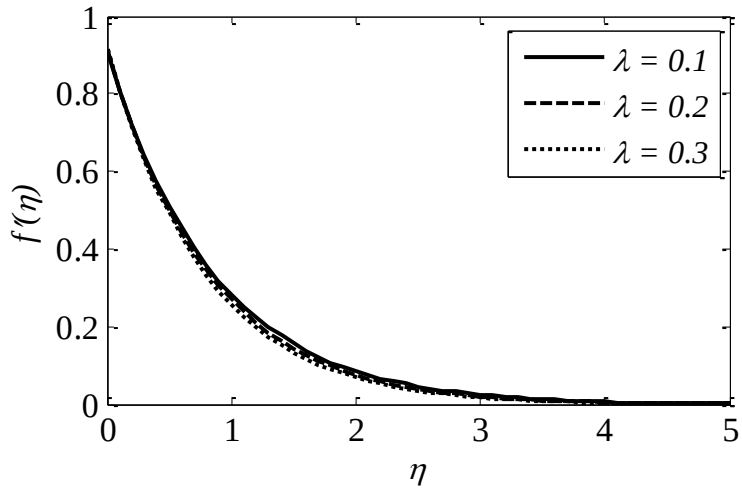

Fig. 4. Effect of λ on velocity profile

Figure 5 illustrates the impact thermal buoyancy factor λ_t has on the velocity. When is λ_t raised, the velocity also improves. This is because buoyancy, affects particles of fluid as a result of gravitational force and in turn boosts the fluid's velocity.

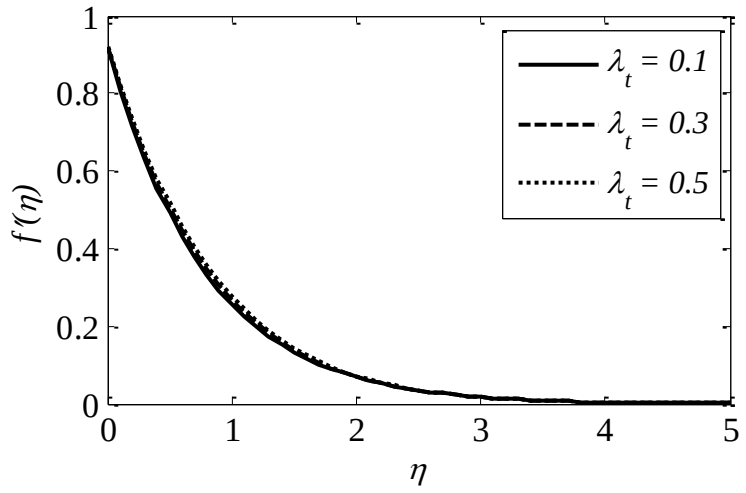

Fig. 5. Effect of λ_t on velocity profile

Expanding the solutal buoyancy factor λ_c, which is apparent in Figure 6, improves the velocity profile. The buoyancy parameter, in a physical sense, lowers the viscous forces that trigger the velocity to go up.

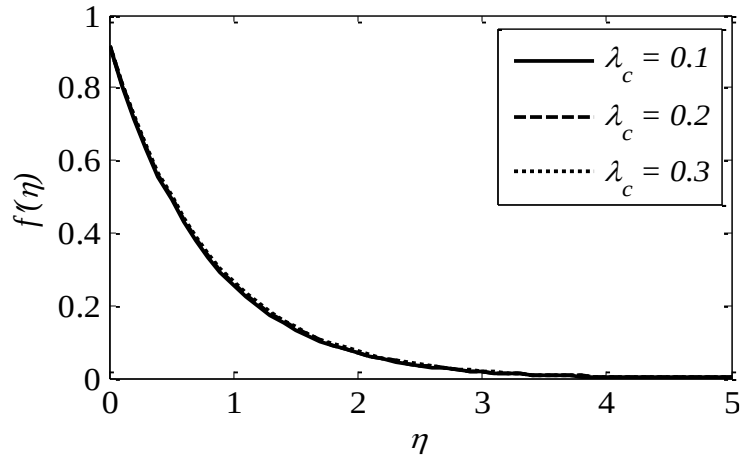

Fig. 6. Effect of λ_c on velocity profile

The velocity profile changes due to suction parameter S are shown in Figure 7. As S parameter increases, the velocity trend appears to be dropping, indicating the common fact that suction maintains the boundary layer's growth and consequently reduces the formation of the highest points in the velocity outline.

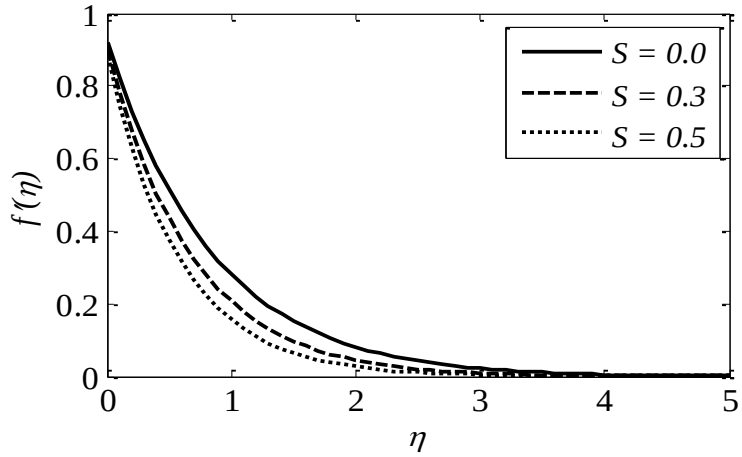

Fig. 7. Effect of S on velocity profile

Figure 8 shows how velocity profile changes with angle of inclination Ω. The Lorentz force escalates with angle of inclination because magnetic fields affect fluid particles more. So, velocity profile drops. For $\Omega = 0$, the magnetic field has no influence on the speed profile, and for $\Omega = \pi / 2$ the fluid particles encounter the greatest possible resistance.

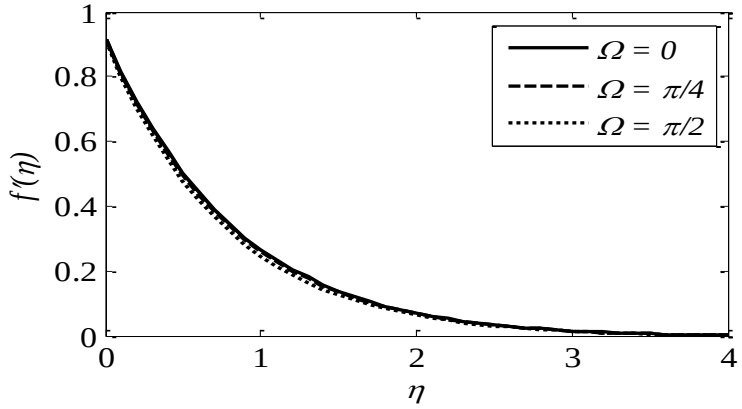

Fig. 8. Effect of Ω on velocity profile

Figure 9 depicts the impacts of surface slip ε on the velocity. Close to the wall, higher readings of the slip parameter cause a reduction of velocity, whereas the reverse is true further from the wall. The asymptotic pattern of velocity to 1 is found in the no-slip $(\varepsilon = 0)$ situation.

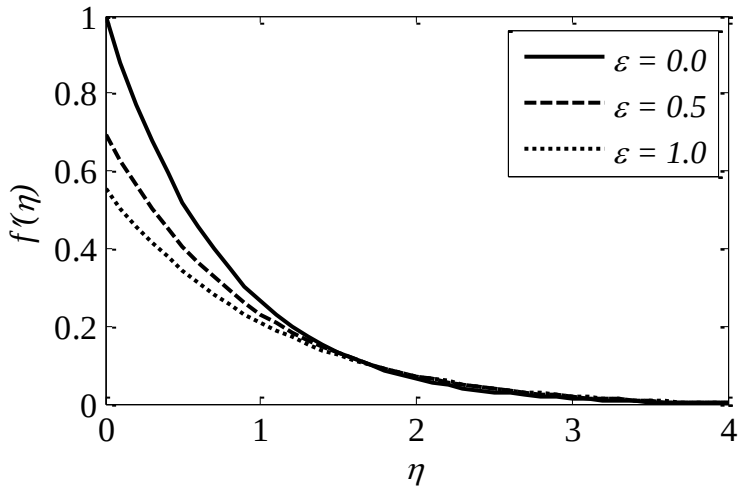

Fig. 9. Effect of ε on velocity profile

Figure 10 implies thermal relaxation parameter γ_e-dependent temperature fluctuation. In close proximity to the surface, the increased heat flow relaxation time raises the temperature and lengthens the thermal boundary layer, while the opposite is true in deeper layers. When thermal relaxation parameter $\gamma_e = 0$, the model approaches Fourier's law.

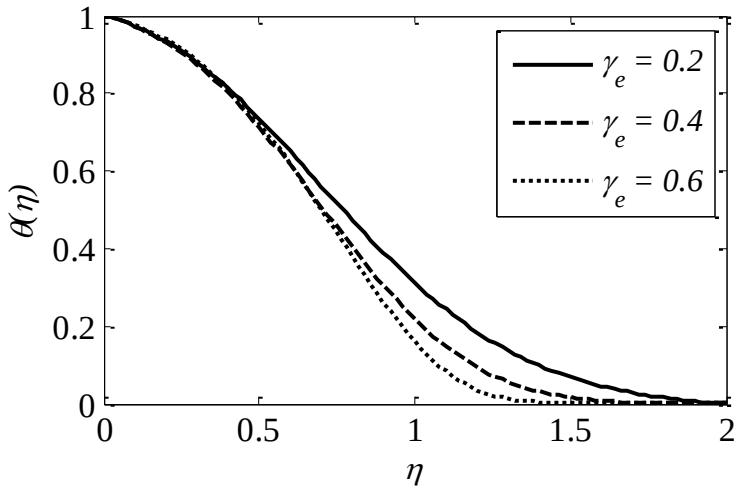

Fig. 10. Effect of γ_e on temperature profile

Figure 11 exhibits the way Prandtl number Pr determines fluid temperature. Pr diminishes fluid temperature. Thermal boundary layer thickness falls further. For stronger Pr, thermal diffusivity shrinks, lowering temperature and boundary layer thickness.

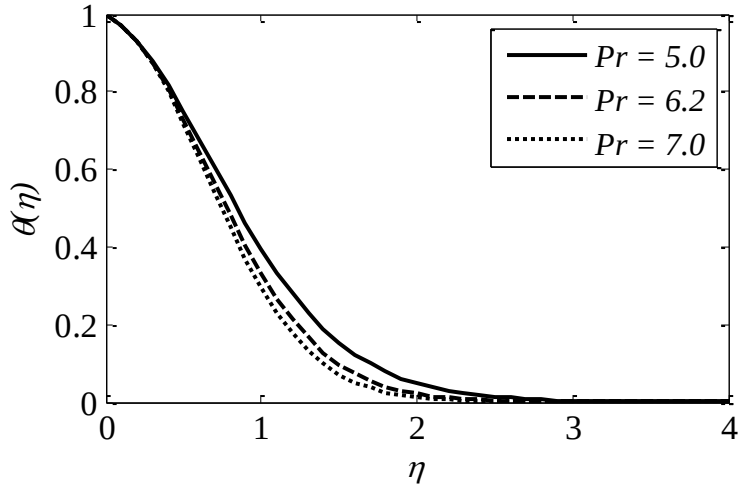

Fig. 11. Effect of $\Pr$ on temperature profile

In Figure 12, we can see how the radiation parameter R affects the overall temperature pattern. When the R value goes up, the temperature profile goes up too. This is because the Fluid has become hotter than usual because of the R.

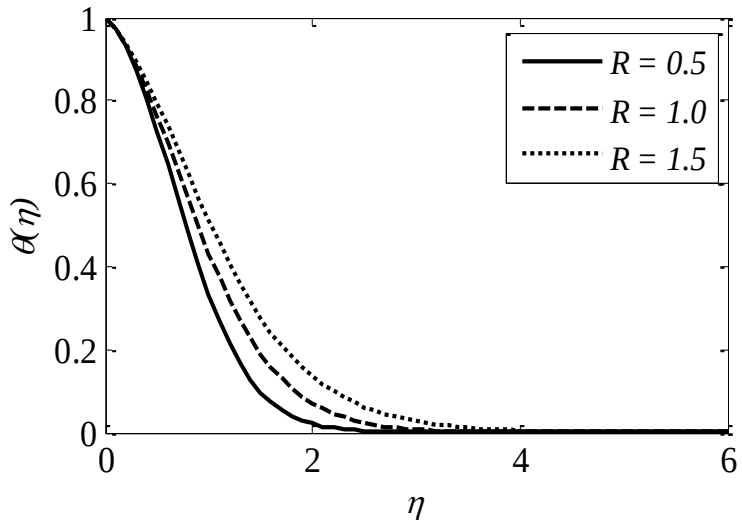

Fig. 12. Effect of R on temperature profile

Figure 13 clarifies the way the heat generation parameter Q governs temperature distribution. Heat generation parameter promotes temperature distribution while heat absorption parameter minimizes it.

Figure 14 and 15 show how the Brownian motion factor Nb modifies temperature and concentration curves. The wider range of Nb boosts nanoparticle kinetic energy, allowing more particles to transition beyond the surface, resulting in higher temperatures but lessening concentration.

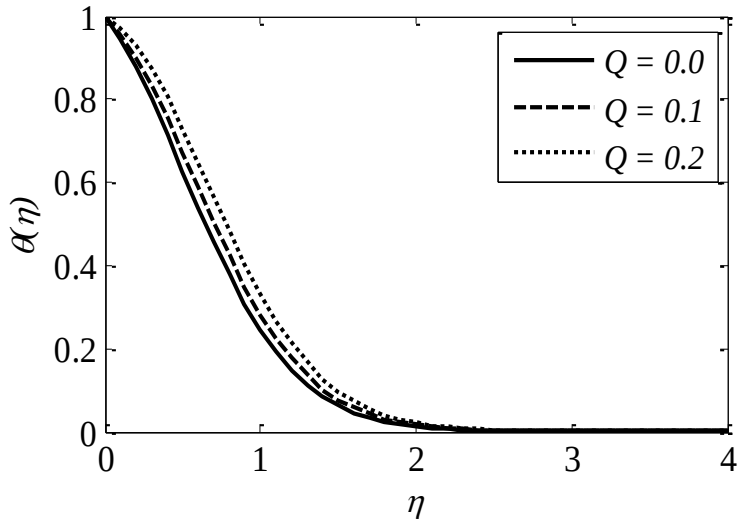

Fig. 13. Effect of Q on temperature profile

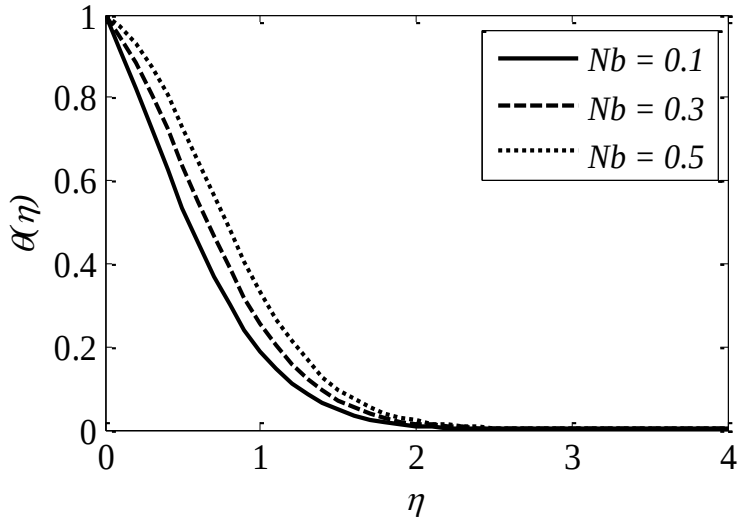

Fig. 14. Effect of Nb on temperature profile

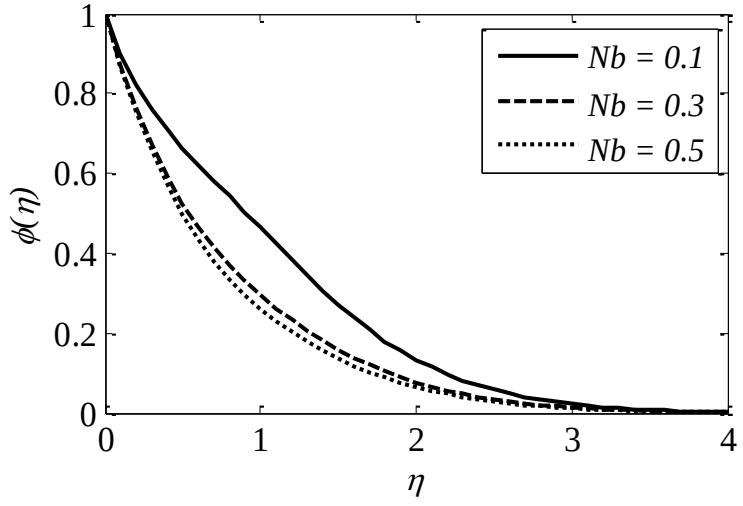

Fig. 15. Effect of Nb on concentration profile

Thermophoresis factor Nt modifies temperature and concentration patterns in Figure 16 and 17. The thermophoresis force drives nanoparticles from hot to cold, evolving the temperature profile. Also Nt alters concentration profile similarly.

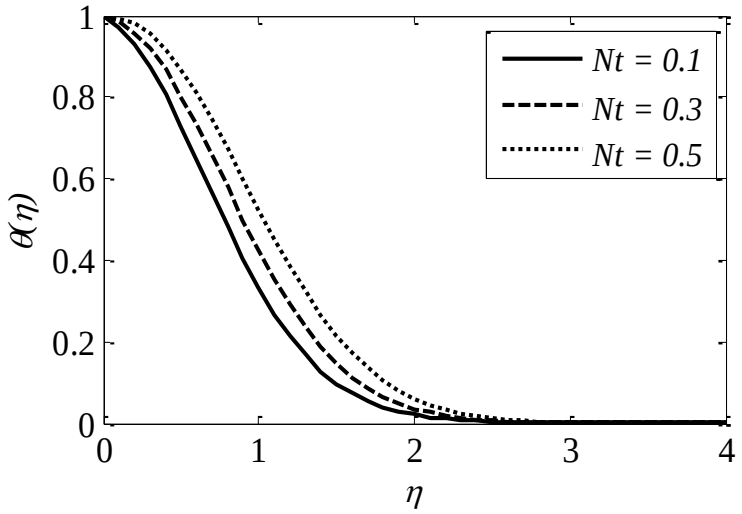

Fig. 16. Effect of Nt on temperature profile

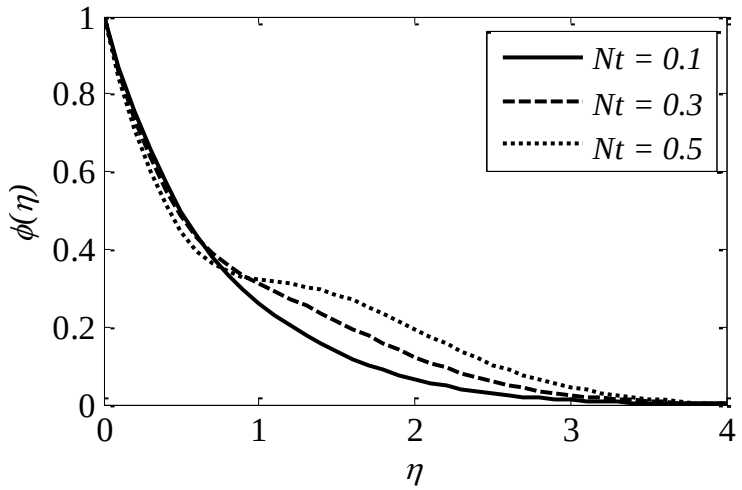

Fig. 17. Effect of Nt on concentration profile

Concentration curves drop with a rise in concentration relaxation parameter γ_c. This is depicted in Figure 18.

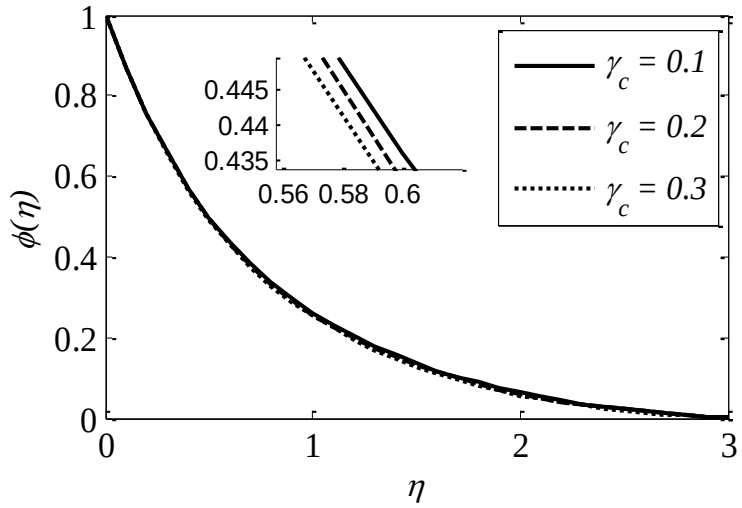

Fig. 18. Effect of γ_c on concentration profile

Figure 19 shows how the Schmidt number Sc alters concentration profiles. As Sc values rise, however, concentration tends downward. The concentration and the corresponding thickness of the concentration boundary layer both reduce as the Sc expands, which makes physical sense. Concentration and the thickness of the concentration boundary layer decline as Sc grows, as would be expected from a physical perspective.

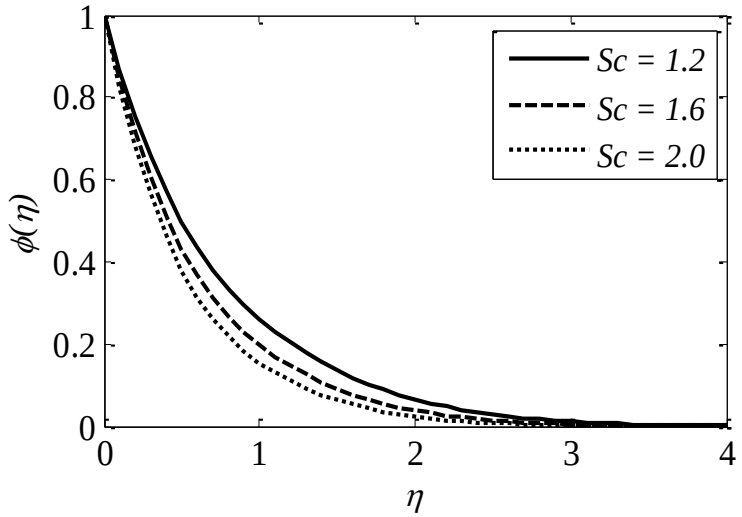

Fig. 19. Effect of Sc on concentration profile

In Figure 20, we look into how the parameter C_r in a chemical process alters the concentration of nanoparticles. As the repercussions of a chemical reaction grows the concentration profile diminishes. When a chemical reaction takes place, the rate of intermolecular mass transfer rises, resulting in a volume reduction of the nanoparticles.

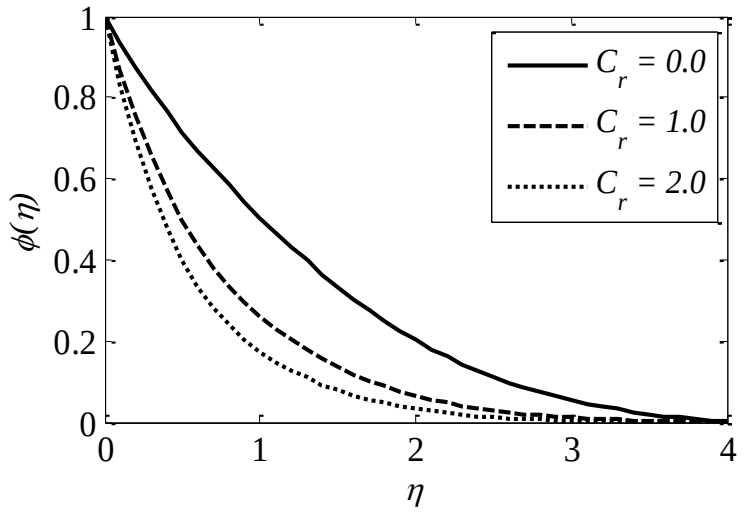

Fig. 20. Effect of C_r on concentration profile

Figure 21 illustrates the manner in which ε and λ alter - $f''(0)$. The figure shows that λ's rising values raise $f''(0)$, but ε reduces it greatly.

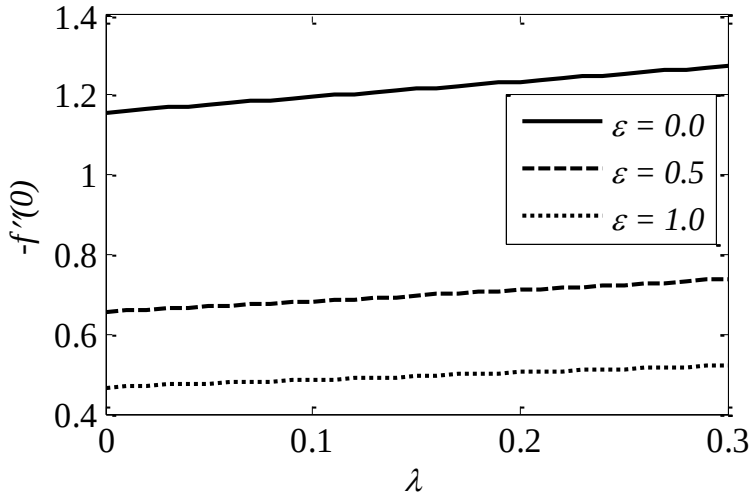

Fig. 21. Effect of λ and ε on $-f''(0)$

Figure 22 demonstrates the ways λ and Q alter Nusselt number. The magnitude value Nu_x lessens as λ and Q evolve.

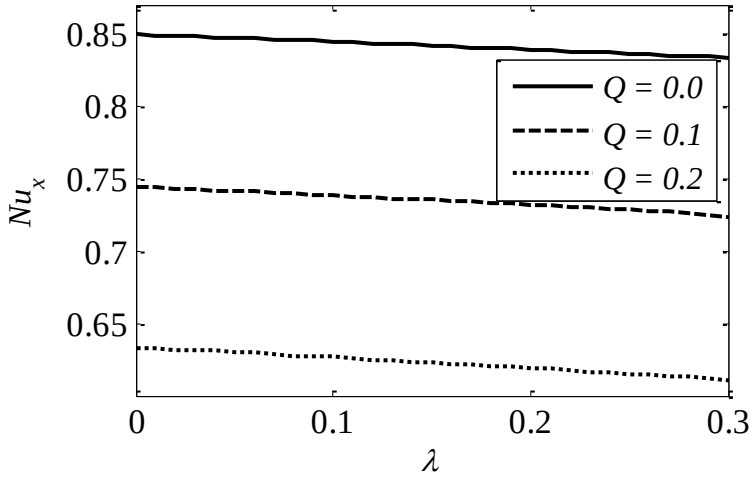

Fig. 22. Effect of λ and Q on Nu_x

Figure 23 illustrates the manner in which C_r and λ alter Sh_x. The figure shows that λ's rising values diminish Sh_x, but C_r accelerates it greatly.

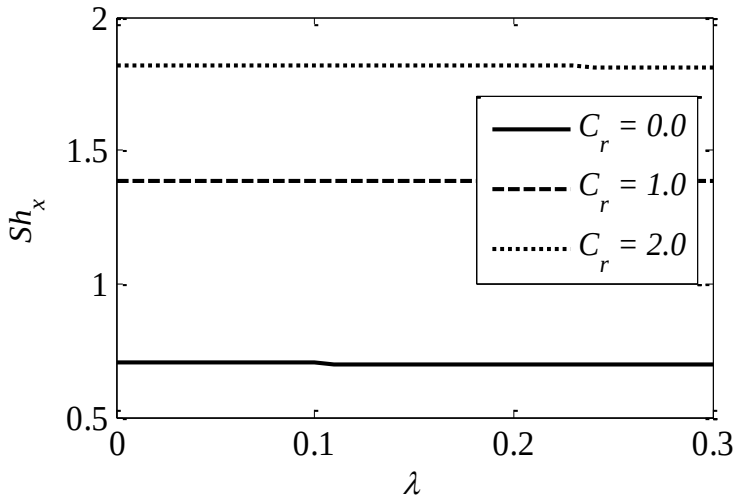

Fig. 23. Effect of λ and C_r on Sh_x

5. Conclusions

This study aims to investigate the phenomenon of upper-convected Maxwell (UCM) nanofluid flow caused by an inclined stretching sheet passing through a magnetic field. The modelling methodology incorporates Cattaneo and Christov's diffusion model for mass and heat transmission. The following are the primary conclusions:

i. Velocity declines with the enhancing values of M, S and λ.
ii. Magnetic parameter M upsurge its temperature profiles.
iii. Heat flow relaxation time at the surface elevates temperature.
iv. Temperature field decays for higher values of $\Pr$, Q.
v. Concentration curves drop with a rise in concentration relaxation parameter.
vi. Temperature rises with the radiation parameter R.

vii. The thermophoresis parameter elevates as a function of both the temperature and concentration patterns.
viii. Greater Maxwell parameters implies a rise in the intensity of skin friction, whereas a spike in the slip parameter generates a decrease.
ix. Nusselt and Sherwood numbers diminish with Maxwell parameter.

Acknowledgement
We appreciate the reviewers' spending the time and making the effort to read the manuscript. We sincerely thank you for your insightful comments and recommendations, which allowed us to increase the manuscript's quality.

Conflict of interests
The authors declare that there is no conflict of interests regarding the publication of this paper.

References
[1] Hwang, Yu-jin, J. K. Lee, C. H. Lee, Y. M. Jung, S. I. Cheong, C. G. Lee, B. C. Ku, and S. P. Jang. "Stability and thermal conductivity characteristics of nanofluids." *Thermochimica Acta* 455, no. 1-2 (2007): 70-74. https://doi.org/10.1016/j.tca.2006.11.036
[2] Jalili, Bahram, Amirhossein Rezaeian, Payam Jalili, Fathollah Ommi, and Davood Domiri Ganji. "Numerical modeling of magnetic field impact on the thermal behavior of a microchannel heat sink." *Case Studies in Thermal Engineering* 45 (2023): 102944. https://doi.org/10.1016/j.csite.2023.102944
[3] Arshad, Mubashar, Azad Hussain, Ali Hassan, Syed Amir Ghazi Ali Shah, Mohamed Abdelghany Elkotab, Soumaya Gouadria, Mishal Alsehli, and Ahmed M. Galal. "Heat and mass transfer analysis above an unsteady infinite porous surface with chemical reaction." *Case Studies in Thermal Engineering* 36 (2022): 102140. https://doi.org/10.1016/j.csite.2022.102140
[4] Jalili, Bahram, Amirhossein Rezaeian, Payam Jalili, Davood Domeri Ganji, and Yasir Khan. "Squeezing flow of Casson fluid between two circular plates under the impact of solar radiation." *ZAMM-Journal of Applied Mathematics and Mechanics/Zeitschrift für Angewandte Mathematik und Mechanik* (2023): e202200455. https://doi.org/10.1002/zamm.202200455
[5] Anwar, Muhammad Imran, Hina Firdous, A. Al Zubaidi, Nadeem Abbas, and Sohail Nadeem. "Computational analysis of induced magnetohydrodynamic non-Newtonian nanofluid flow over nonlinear stretching sheet." *Progress in Reaction Kinetics and Mechanism* 47 (2022): 14686783211072712. https://doi.org/10.1177/14686783211072712
[6] Esfe, Mohammad Hemmat, and Masoud Afrand. "An updated review on the nanofluids characteristics: Preparation and measurement methods of nanofluids thermal conductivity." *Journal of Thermal Analysis and Calorimetry* 138, no. 6 (2019): 4091-4101. https://doi.org/10.1007/s10973-019-08406-2
[7] Reddy, P. Sudarsana, and P. Sreedevi. "Impact of chemical reaction and double stratification on heat and mass transfer characteristics of nanofluid flow over porous stretching sheet with thermal radiation." *International Journal of Ambient Energy* 43, no. 1 (2022): 1626-1636. https://doi.org/10.1080/01430750.2020.1712240
[8] Motsa, S. S., T. Hayat, and O. M. Aldossary. "MHD flow of upper-convected Maxwell fluid over porous stretching sheet using successive Taylor series linearization method." *Applied Mathematics and Mechanics* 33 (2012): 975-990. https://doi.org/10.1007/s10483-012-1599-x
[9] Shateyi, S., and G. T. Marewo. "A new numerical approach of MHD flow with heat and mass transfer for the UCM fluid over a stretching surface in the presence of thermal radiation." *Mathematical Problems in Engineering* 2013 (2013). https://doi.org/10.1155/2013/670205
[10] Hayat, T., M. Mustafa, S. A. Shehzad, and S. Obaidat. "Melting heat transfer in the stagnation-point flow of an upper-convected Maxwell (UCM) fluid past a stretching sheet." *International Journal for Numerical Methods in Fluids* 68, no. 2 (2012): 233-243. https://doi.org/10.1002/fld.2503
[11] Kodi, Raghunath, Charankumar Ganteda, Abhishek Dasore, M. Logesh Kumar, G. Laxmaiah, Mohd Abul Hasan, Saiful Islam, and Abdul Razak. "Influence of MHD mixed convection flow for maxwell nanofluid through a vertical cone with porous material in the existence of variable heat conductivity and diffusion." *Case Studies in Thermal Engineering* 44 (2023): 102875. https://doi.org/10.1016/j.csite.2023.102875

[12] Ahmadi, Mohammad Hossein, Amin Mirlohi, Mohammad Alhuyi Nazari, and Roghayeh Ghasempour. "A review of thermal conductivity of various nanofluids." *Journal of Molecular Liquids* 265 (2018): 181-188. https://doi.org/10.1016/j.molliq.2018.05.124
[13] Khan, Yasir, Qingbiao Wu, Naeem Faraz, Ahmet Yıldırım, and Syed Tauseef Mohyud-Din. "Heat transfer analysis on the magnetohydrodynamic flow of a non-Newtonian fluid in the presence of thermal radiation: an analytic solution." *Zeitschrift für Naturforschung A* 67, no. 3-4 (2012): 147-152. https://doi.org/10.5560/zna.2012-0001
[14] Shah, Sajid, Shahzada M. Atif, and Abid Kamran. "Radiation and slip effects on MHD Maxwell nanofluid flow over an inclined surface with chemical reaction." *Heat Transfer* 50, no. 4 (2021): 4062-4085. https://doi.org/10.1002/htj.22064
[15] Das, Kalidas. "Slip effects on heat and mass transfer in MHD micropolar fluid flow over an inclined plate with thermal radiation and chemical reaction." *International Journal for Numerical Methods in Fluids* 70, no. 1 (2012): 96-113. https://doi.org/10.1002/fld.2683
[16] Raghunath, Kodi. "Study of Heat and Mass Transfer of an Unsteady Magnetohydrodynamic (MHD) Nanofluid Flow Past a Vertical Porous Plate in the Presence of Chemical Reaction, Radiation and Soret Effects." *Journal of Nanofluids* 12, no. 3 (2023): 767-776. https://doi.org/10.1166/jon.2023.1965
[17] Ali, Bagh, Yufeng Nie, Shahid Ali Khan, Muhammad Tariq Sadiq, and Momina Tariq. "Finite element simulation of multiple slip effects on MHD unsteady maxwell nanofluid flow over a permeable stretching sheet with radiation and thermo-diffusion in the presence of chemical reaction." *Processes* 7, no. 9 (2019): 628. https://doi.org/10.3390/pr7090628
[18] Raftari, Behrouz, and Ahmet Yildirim. "The application of homotopy perturbation method for MHD flows of UCM fluids above porous stretching sheets." *Computers & Mathematics with Applications* 59, no. 10 (2010): 3328-3337. https://doi.org/10.1016/j.camwa.2010.03.018
[19] Farooq, Umer, Dianchen Lu, Shahzad Munir, Muhammad Ramzan, Muhammad Suleman, and Shahid Hussain. "MHD flow of Maxwell fluid with nanomaterials due to an exponentially stretching surface." *Scientific Reports* 9, no. 1 (2019): 7312. https://doi.org/10.1038/s41598-019-43549-0
[20] Ibrahim, Wubshet, and Mekonnen Negera. "MHD slip flow of upper-convected Maxwell nanofluid over a stretching sheet with chemical reaction." *Journal of the Egyptian Mathematical Society* 28, no. 1 (2020): 7. https://doi.org/10.1186/s42787-019-0057-2
[21] Hayat, T., and M. Awais. "Three-dimensional flow of upper-convected Maxwell (UCM) fluid." *International Journal for Numerical Methods in Fluids* 66, no. 7 (2011): 875-884. https://doi.org/10.1002/fld.2289
[22] Tausif, Sk Md, K. Das, and P. K. Kundu. "Modified Homogeneous and Heterogeneous Chemical Reaction and Flow Performance of Maxwell Nanofluid with Cattaneo-Christov Heat Flux Law." *Journal of Engineering Thermophysics* 31, no. 1 (2022): 64-77. https://doi.org/10.1134/S1810232822010064
[23] Nandeppanavar, Mahantesh M., M. C. Kemparaju, and M. Subhas Abel. "Thermal radiative MHD stagnation point slip flow and heat transfer due to a stretching sheet." *Journal of Nanofluids* 7, no. 2 (2018): 350-357. https://doi.org/10.1166/jon.2018.1453
[24] Narender, G., K. Govardhan, and G. Sreedhar Sarma. "Mhd stagnation point casson nanofluid flow over a radially stretching sheet." *Beilstein Archives* 2019, no. 1 (2019): 137. https://doi.org/10.3762/bxiv.2019.137.v1
[25] Awan, Aziz Ullah, Sana Abid, Naeem Ullah, and Sohail Nadeem. "Magnetohydrodynamic oblique stagnation point flow of second grade fluid over an oscillatory stretching surface." *Results in Physics* 18 (2020): 103233. https://doi.org/10.1016/j.rinp.2020.103233
[26] Kumar, Ravinder, Rakesh Kumar, K. Vajravelu, and M. Sheikholeslami. "Three dimensional stagnation flow of Casson nanofluid through Darcy-Forchheimer space: a reduction to Blasius/Sakiadis flow." *Chinese Journal of Physics* 68 (2020): 874-885. https://doi.org/10.1016/j.cjph.2020.10.027
[27] Hosseinzadeh, Kh, M. Gholinia, B. Jafari, A. Ghanbarpour, H. Olfian, and D. D. Ganji. "Nonlinear thermal radiation and chemical reaction effects on Maxwell fluid flow with convectively heated plate in a porous medium." *Heat Transfer-Asian Research* 48, no. 2 (2019): 744-759. https://doi.org/10.1002/htj.21404
[28] Patil, Amar B., Vishwambhar S. Patil, Pooja P. Humane, Nalini S. Patil, and Govind R. Rajput. "Thermally and chemically reacted MHD Maxwell nanofluid flow past an inclined permeable stretching surface." *Proceedings of the Institution of Mechanical Engineers, Part E: Journal of Process Mechanical Engineering* 236, no. 3 (2022): 838-848. https://doi.org/10.1177/09544089211050715
[29] Mustafa, M., T. Hayat, and A. Alsaedi. "Rotating flow of Maxwell fluid with variable thermal conductivity: an application to non-Fourier heat flux theory." *International Journal of Heat and Mass Transfer* 106 (2017): 142-148. https://doi.org/10.1016/j.ijheatmasstransfer.2016.10.051
[30] Sheikholeslami, Mohsen. "Effect of uniform suction on nanofluid flow and heat transfer over a cylinder." *Journal of the Brazilian Society of Mechanical Sciences and Engineering* 37 (2015): 1623-1633. https://doi.org/10.1007/s40430-014-0242-z

[31] Shah, Nehad Ali, I. L. Animasaun, Abderrahim Wakif, O. K. Koriko, R. Sivaraj, K. S. Adegbie, Zahra Abdelmalek, H. Vaidyaa, A. F. Ijirimoye, and K. V. Prasad. "Significance of suction and dual stretching on the dynamics of various hybrid nanofluids: Comparative analysis between type I and type II models." *Physica Scripta* 95, no. 9 (2020): 095205. https://doi.org/10.1088/1402-4896/aba8c6

[32] Azam, Muhammad. "Effects of Cattaneo-Christov heat flux and nonlinear thermal radiation on MHD Maxwell nanofluid with Arrhenius activation energy." *Case Studies in Thermal Engineering* 34 (2022): 102048. https://doi.org/10.1016/j.csite.2022.102048

[33] Omowaye, Adeola John, and Isaac Lare Animasaun. "Upper-convected maxwell fluid flow with variable thermo-physical properties over a melting surface situated in hot environment subject to thermal stratification." *Journal of Applied Fluid Mechanics* 9, no. 4 (2016): 1777-1790. https://doi.org/10.18869/acadpub.jafm.68.235.24939

[34] Shah, Sajid, Shahzada M. Atif, and Abid Kamran. "Radiation and slip effects on MHD Maxwell nanofluid flow over an inclined surface with chemical reaction." *Heat Transfer* 50, no. 4 (2021): 4062-4085. https://doi.org/10.1002/htj.22064